IBRACON Structures and Materials Journal
Revista IBRACON de Estruturas e Materiais
ISSN 1983-4195 ismj.org

ORIGINAL ARTICLE

# Dynamic identification of a cable-stayed footbridge using a low-cost data acquisition system

## *Identificação dinâmica de uma passarela estaiada utilizando um sistema de aquisição de dados de baixo custo*

Danilo de Santana Nunes[a]
José Luis Vital de Brito[b]
Graciela Nora Doz[b]

[a]Universidade Estadual de Santa Cruz - UESC, Departamento de Engenharias e Computação, Ilhéus, BA, Brasil
[b]Universidade de Brasília - UnB, Programa de Pós-graduação em Estruturas e Construção Civil, Brasília, DF, Brasil

Received 19 October 2022
Accepted 23 February 2023

**Abstract:** This study describes the dynamic identification of a cable-stayed footbridge using an alternative data acquisition system and output-only modal identification methods. Data were collected during dynamic tests performed using an acquisition system based on the Arduino platform, consisting of low-cost devices with on-board Micro-Electro-Mechanical System (MEMS) accelerometers. The Peak-Picking (PP) method was used for the stay cables. The Frequency Domain Decomposition (FDD) and Stochastic Subspace Identification – Unweighted Principal Components (SSI-UPC) methods were used for the complete structure. The proposed data acquisition system efficiently recorded the time series required for Operational Modal Analysis and the acceleration acquisition process provided stable results. At least four mode shapes were identified in all tests. A minimum of four high energy peaks in the 0 – 24 Hz frequency range of the spectrum were obtained by the acquisition system in all of the cable tests and selected by the method. In the complete structure tests, the low-cost data acquisition system and the identification methods provided the first four flexural mode shapes, within the 0 – 9 Hz frequency range. Results for the frequency domain method showed a maximum difference of 2.37% in the first experimental frequency when compared to a 3D finite element numerical model, while in the other frequencies the difference was between 1 and 2%. For the time domain method, the maximum difference was 1.74% in the fourth frequency, with differences of between 0.1 and 0.7% in the other frequencies. The mode shapes were evaluated using the Modal Assurance Criterion (MAC) index, and the results varied between 0.8513 and 0.9990.

**Keywords:** cable-stayed footbridge, data acquisition system, modal identification, dynamic tests, low-cost devices.

**Resumo:** Este trabalho apresenta a identificação dinâmica de uma passarela estaiada a partir da aplicação de um sistema de aquisição de dados alternativo e métodos de identificação modal que se baseiam apenas na resposta. Os dados foram coletados durante ensaios dinâmicos realizados com um sistema de aquisição baseado na plataforma Arduino, composto por dispositivos de baixo custo com acelerômetros microeletromecânicos embarcados. Para os estais, foi utilizado o método *Peak-Picking*. Para a estrutura completa, foram utilizados os métodos *Frequency Domain Decomposition* e o *Stochastic Subspace Identification – Unweighted Principal Components*. O sistema de aquisição de dados proposto registrou as séries temporais necessárias para a Análise Modal Operacional de forma eficiente e o processo de aquisição das acelerações proporcionou resultados estáveis. Pelo menos quatro formas modais foram identificadas em todos os testes. Em todos os ensaios dos estais, um mínimo de quatro picos de alta energia na faixa de frequência entre 0 – 24 Hz do espectro foram obtidos com o sistema de aquisição e selecionados pelo método. Nos ensaios da estrutura completa, o sistema de aquisição de dados de baixo custo e os métodos de identificação forneceram os quatro primeiros modos de flexão, dentro da faixa de frequência entre 0 – 9 Hz. Os resultados do método no domínio da frequência mostraram uma diferença máxima, quando comparados aos de um modelo numérico 3D em elementos finitos, de 2,37% na primeira frequência experimental, enquanto que nas demais frequências a diferença ficou entre 1 e 2%. Para o método no domínio do tempo, a diferença máxima foi de 1,74% na quarta frequência, enquanto que nas demais, a diferença ficou entre 0,1 e

**Corresponding author:** Danilo de Santana Nunes. E-mail: dsnunes@uesc.br
**Financial support:** None.
**Conflict of interest:** Nothing to declare.
**Data Availability:** The data that support the findings of this study are available from the corresponding author, [D. de S.], upon reasonable request.

0,7%. As formas modais foram avaliadas através do índice *Modal Assurance Criterion*, e os resultados variaram entre 0,8513 e 0,9990.

**Palavras-chave:** passarela estaiada, sistema de aquisição de dados, identificação modal, ensaios dinâmicos, dispositivos de baixo custo.

**How to cite:** D. S. Nunes, J. L. V. Brito, and G. N. Doz, "Dynamic identification of a cable-stayed footbridge using a low-cost data acquisition system," *Rev. IBRACON Estrut. Mater.*, vol. 16, no. 6, e16610, 2023, https://doi.org/10.1590/S1983-41952023000600010

## 1 INTRODUCTION

Bridge maintenance, safeguarding, and health monitoring are important topics in the prevention of potentially catastrophic events [1]. Analysis generally involves accurate numerical modeling of the structure, which must be calibrated, usually for the material parameters and boundary conditions, according to the on-site response to the dynamic loads [2]. Modal parameters estimated from the data obtained via nondestructive tests, usually ambient vibration tests, can be used in the structural model updating and Structural Health Monitoring (SHM) processes. The dynamic properties are also useful for model updating [3] and provide a good evaluation tool for non-destructive damage assessment [4]. As such, buildings and other structures (e.g., bridges, highways, etc.) have been equipped with monitoring systems that provide continuous control, thus minimizing the possibility of structural hazards [5]. The usual sensing techniques used in SHM include piezoelectric transducers, Macro Fiber Composites, optic Fiber Bragg Grating sensors, accelerometers, strain gauges, acoustic emission sensors, etc. [6], but new ideas have been proposed for recording the dynamic response of structures [7]. Novel sensing technologies, high-speed computing, and communication technologies could enable the engineering community to measure and evaluate ambient structural vibrations quickly and accurately [8].

Both the traditional and innovative systems have advantages and disadvantages. The traditional systems are composed of acquisition boards and signal conditioners that offer the best performance to date, using analog sensors that offer high sensitivity and low signal noise. The most recent systems mainly pursue wireless solutions in order to eliminate interruptions to the structures' operations, as well as provide continuous and remote monitoring of the structure, as described in [9], [10]. It would be much less expensive to use low-cost sensors for this purpose that can remain fixed to or embedded in the structure (not recovered), as long as they offer acceptable performance and robustness. The digital sensors known as Micro-Electro-Mechanical Systems (MEMS) display these characteristics. The benefits of these sensors include their small size, low weight, high performance, easy mass production, low cost [11], and low power consumption, which is an important advantage of battery-powered wireless systems. Their main disadvantage is that they lack the high sensitivity of an analog sensor [5], as well as presenting more output noise. However, despite this, research groups working in a range of fields have obtained promising results with their low-cost systems [12]-[16]. The civil engineering area could also benefit from this technology, which has become increasingly accessible with the growth of electronic prototyping platforms such as the Arduino platform. The Arduino devices, boards, and sensors providing interesting commercial alternatives for these types of applications [17].

Arduino boards can read inputs and turn them into an output. The board can be controlled via a set of instructions sent to its microcontroller, using the Arduino programming language [18] and the Arduino Integrated Development Environment (IDE) [19], [20]. This enables the creation of tools capable of high-resolution environmental monitoring without a large financial investment and with minimal development effort or experience. Additionally, the Arduino boards have demonstrated that they are capable of withstanding a large amount of physical abuse [21]. This physical resistance demonstrates their capacity for use in the application of continuous health monitoring of civil structures [17]. The option selected for this research was the Arduino/Genuino 101 board (a low-cost device), equipped with the Bosch BMI160 3-axis accelerometer and gyroscope, and the open software Realterm [22] to capture and register the acceleration time series. This paper focuses on the dynamic properties identification of a cable-stayed footbridge via the application of output-only modal identification methods, using the data collected with a low-cost data acquisition system. This is the first step in the integrity evaluation process of cable-stayed structures, which would follow these steps: *i*) dynamic testing of the stay cables and complete structure using a low-cost data acquisition system; *ii*) identification of the natural frequencies of the stays using a dynamic identification method, in order to determine the prestressing forces through the Mersenne/Taylor Law; *iii*) identification of the dynamic properties (natural frequencies and modes of vibration) of the structure using stochastic modal identification methods, given the difficulty of using deterministic excitations and even interrupting the operation of infrastructure constructions, as is the case with cable-stayed structures (bridges and footbridges); *iv*) design and updating of the numerical model of the structure by inserting the experimental prestressing forces of the stays into the numerical model and optimization of the materials properties

process; *v*) analysis of the current efforts of the structure, provided by the updated numerical model, in comparison with the structural design, so as to identify overloaded regions; *vi*) new testing and updating stages at pre-defined age intervals, using the updated numerical model as a reference, in order to identify any variations in the dynamic properties and stay forces that could characterize a change in the stiffness and equilibrium condition of the structure, indicating structural problems in service. The methods and computational systems used in the first three steps, which were the objective of this research, are presented below in detail.

## 2 DYNAMIC STRUCTURAL IDENTIFICATION

Three methods were used for dynamic identification, two in the frequency domain and one in the time domain. The cable tests used one sensor to determine only the natural frequencies of the system, using the frequency domain Peak-Picking (PP) Method. The complete structure tests used three sensors and 17 setups, which enabled the mode shapes to be obtained using the Frequency Domain Decomposition (FDD) and the Stochastic Subspace Identification – Unweighted Principal Components (SSI-UPC) methods.

### 2.1 Peak-Picking Method (PP)

The structure's natural frequencies are associated with the values of frequency peaks, where the amplitude tends to infinity in the Frequency Response Function (FRF) and in the power spectrum estimated using the Fast Fourier Transform (FFT). Equation 1 shows the FFT applied to the signal $R(\tau)$, resulting in the power spectrum $S(f)$.

$$S(f) = \int_{-\infty}^{\infty} R(\tau) e^{-i2\pi f\tau}\, d\tau \tag{1}$$

For multiple degrees of freedom, the spectral information can be organized into matrices as shown in Equation 2:

$$S_q(f) = H(f)\, S_p(f)\, H^H(f) \tag{2}$$

where $S_q(f)$ = Power Spectral Density (PSD) functions matrix of response; $H(f)$ = FRFs matrix; $H^H(f)$ = transposed conjugate of matrix $H(f)$; and $S_p(f)$ = PSD functions matrix of excitation.

### 2.2 Frequency Domain Decomposition Method (FDD)

The FDD also uses the PSD functions of the response and adopts the following steps:

*i*) Calculation and evaluation of the normalized PSD functions of the response: Normalization is an artifice used to overcome certain drawbacks when working with several measurement setups, such as the greatest number of degrees of freedom. This provides a higher number of frequency peaks of each auto-spectrum to be identified, and the variation in excitation intensity during the test, which leads to different energy contents for the measured time series. Thus, it is sought to normalize the energy content of each spectrum, which can be performed by dividing each ordinate of the $PSD_i(\omega)$ function by summation of all ordinates $N$, resulting in a normalized function ($NPSD_i(\omega)$), as follows:

$$NPSD_i(\omega) = \frac{PSD_i(\omega)}{\sum_{k=1}^{N} PSD_i(\omega_k)} \tag{3}$$

Through Equation 3, we achieve equality between the areas under each spectrum. The next step is to determinate the average $NPSD_i(\omega)$, the $ANPSD$ functions, by Equation 4:

$$ANPSD = \frac{1}{setups} \sum_{i=1}^{setups} NPSD_i\,(\omega) \tag{4}$$

*ii*) Singular Value Decomposition (SVD) of the average normalized PSD functions matrix;

*iii*) Peak selection of the average normalized PSD decomposed in singular values, which correspond to the structure's natural frequencies;
*iv*) Evaluation of mode shapes through the singular vectors related to the singular values (natural frequencies) obtained at the degrees of freedom (measurement points).

### 2.3 Stochastic Subspace Identification – Unweighted Principal Components Method (SSI-UPC)

Subspace methods identify state-space models from (input and) output data by applying numerical techniques, such as QR factorization and SVD. The discrete-time deterministic state-space model is obtained by Equations 5 and 6:

$$x_{k+1} = Ax_k + Bp_k \tag{5}$$

$$y_k = Cx_k + Dp_k \tag{6}$$

where $x_k$ = discrete-time state vector; $p_k$ = input samples; $y_k$ = output samples; $A$ = discrete system state matrix; $B$ = discrete input matrix; $C$ = output matrix; $D$ = direct transmission matrix.

The SSI-UPC follows these steps:

*i*) Kalman filter application: The aim of the Kalman filter is to produce an optimal prediction, $\hat{X}_i$, for the state vector $x_k$ by making use of observations of the outputs up to time $k$-1 and the available system matrices, together with noise and others uncertainties.
*ii*) Organization of response time series by the Hankel matrix: Reduction of the matrices is performed in the Data-Driven Stochastic Subspace by projecting the row space of the future outputs into the row space of the past reference sensors (outputs). This projection is computed from the QR factorization of a big data Hankel matrix. In addition, this also aims to cancel out the noise.
*iii*) Projection matrix weighting: The data matrices are weighted before the application of the SVD. This weighting determines the state-space basis in which the identified model will be identified. In SSI-UPC, as the term "unweighted" suggests, the weighting matrices $W_1$ and $W_2$ applied to the projection matrix $P_i^{ref}$ are equal to identity matrices $I$ with the same order, as follows (Equation 7):

$$P_{i,w}^{ref} = W_1 P_i^{ref} W_2 \tag{7}$$

where $P_{i,w}^{ref}$ = weighted projection matrix.

Influencing the state vector prediction:

$$\hat{X}_i = O_i^* P_{i,w}^{ref} \tag{8}$$

where $\hat{X}_i$ = optimal state vector prediction; $O_i^*$ = conjugate transpose of the observability matrix.
*iv*) SVD: The decomposition reveals the order of the system and the column space of the observability matrix $O_i$ (Equation 8).
*v*) Identification of system matrices: After applying the numerical techniques described above, the stochastic state-space model representation for multiple degrees of freedom results in Equation 9:

$$\begin{bmatrix} \hat{X}_{i+1} \\ Y_{i/i} \end{bmatrix} = \begin{bmatrix} A \\ C \end{bmatrix} \hat{X}_i + \begin{bmatrix} W_i \\ V_i \end{bmatrix} \tag{9}$$

where $\hat{X}_{i+1}$ = Kalman filter state sequence; $Y_{i/i}$ = Hankel matrix with only one block row; $W_i$ = process noise; and $V_i$ = measurement noise, which is considered as white noise can be excluded from the process because of its constant energy content, resulting in Equation 10:

$$\begin{bmatrix} A \\ C \end{bmatrix} = \begin{bmatrix} \hat{X}_{i+1} \\ Y_{i/i} \end{bmatrix} \hat{X}_i^* \tag{10}$$

where $\hat{X}_i^*$ = conjugate transpose of the $\hat{X}_i$ vector.

The modal parameters of the dynamical system can then be extracted from the state matrix $A$, which contains the matrices of the structure ($M$, $C_1$ and $K$), based on solving an eigenvalues and eigenvectors problem. Equation 11 shows the system matrices:

$$A = \begin{bmatrix} 0 & I \\ -M^{-1}K & -M^{-1}C_1 \end{bmatrix} \tag{11}$$

where $M$ = mass matrix; $C_1$ = damping matrix; and $K$ = stiffness matrix of the structure.

*vi*) Stabilization diagram: Selects stable, unstable and noise modes, thus determining the dimension of the ideal state space. For modes to be classified as stable they must meet certain requirements, e.g., valid range of damping rates. By adjusting this range, harmonic components and non-physical modes can be filtered out, with only true modes of vibration highlighted as stable modes.

More details about the methods presented above can be found in [23] and [24].

## 3 MATERIALS AND EXPERIMENTAL PROGRAM

### 3.1 Data Acquisition System

The acquisition system assembled to perform the dynamic tests of the complete structure consisted of a computer with data acquisition software, three 5.0m-long USB A/B cables, three 15.0m-long USB A/B extension cables equipped with signal amplifiers, and three Arduino/Genuino 101 boards. For the stay cable tests, the acceleration time series were obtained using one Arduino/Genuino 101 board connected to the computer by a 3.0m-long USB A/B cable. Figure 1 shows the components of the data acquisition system.

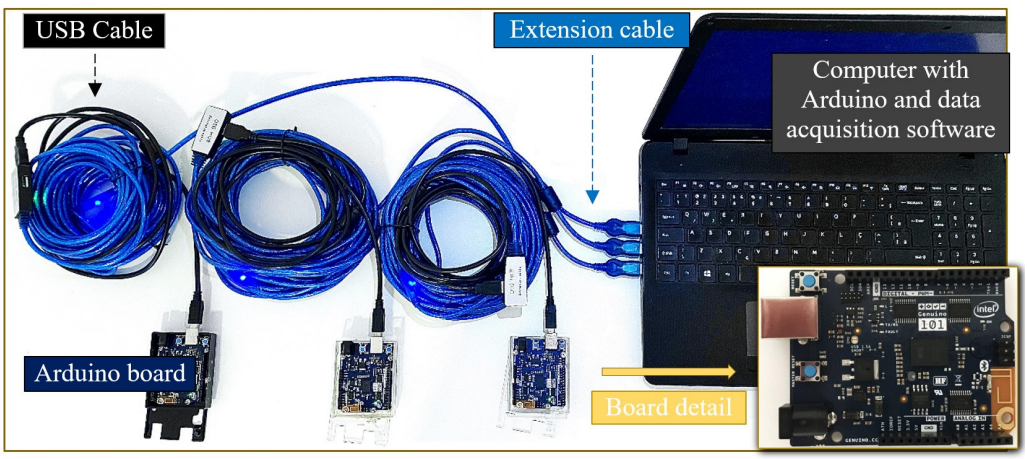


**Figure 1.** Data acquisition system - Arduino boards, cables, extension cables and computer.

The Arduino/Genuino 101 board comes preprogrammed with a Real Time Operating System (RTOS) that handles USB connection and allows new code to be uploaded without the use of an external hardware programmer. It communicates using the device firmware update protocol. It contains the Intel® Curie™ Module, designed to integrate the core's low power consumption and high performance with the Arduino boards. It maintains the same robust form factor and peripheral list as the Arduino UNO basic board version, with the addition of on-board Bluetooth LE capabilities and a 6-axis accelerometer/gyroscope. The RTOS and framework developed by Intel is open sourced. The

board has 14 digital input/output pins, six analog inputs, a USB connector for serial communication and uploading of sketches (which can also be used as a power supply), a power jack, an ICSP header with SPI signals, and I2C dedicated pins [25]. It can be supplied with the following specifications: 7 – 12V (via DC power jack), 7 – 12V (via VIN pin), or 5V (via USB connector), with the latter used in this research. In addition, the board can be powered by an external power supply, which represents an important feature for large structure applications.

To work with the acceleration data it is necessary to implement the "CurieIMU.h" library, which gives access to all the parameters, features and readings of the Arduino/Genuino 101 board's Inertial Measurement Units (IMU) chip. This library is part of the board core and it is loaded together with the core files [25]. Each board was programmed during this research, using the open-source Arduino IDE, to read accelerations at the desired sampling frequency (above 200 Hz) by using the loop function, which repeats the implemented code at the desired time, and with enough output data to obtain the time series (time, accelerations in x, y, and z-axis directions). The Bosch BMI160 3-axis accelerometer and gyroscope contained in the board's IMU chip has ±2 g sensitivity at 16384 LSB/g and 180 μg/√Hz typical output noise. The Arduino/Genuino 101 was chosen for this research because of its practicality for use in real structures. Its compact shape and sturdiness are attractive for applications in the structural engineering field.

Open-source RealTerm software was used to capture and record the accelerations measured by the on-board Bosch BMI160 accelerometer. This serial terminal program is designed for capturing, controlling and debugging binary and other difficult data streams. It automatically identifies and registers any device programmed to perform measurements, simply by selecting the desired USB port. For example, for the tests with three Arduino boards, three USB ports were selected and used simultaneously through three different RealTerm software windows.

The proposed data acquisition system was tested in advance by the research team in the laboratory. Three different structural models were used–a three-story shear building reduced model, a fixed-free bar reduced model, and a concrete slab (6.1 m long, 4.9 m wide and 0.1 m thick)–in four different tests, with one sensor applied in each model (three tests) and two sensors applied with the slab (the fourth test), in order to also identify mode shapes. In the shear building and fixed-free bar tests, which used manually imposed initial displacements to put the models in free vibration, the proposed system's results were compared to a professional system consisting of an accelerometer made by Endevco (model 7754-A), a signal conditioner made by Endveco (model 4416BM1), and a data acquisition module made by Linx (model ADS2000). In the concrete slab tests with one and two sensors, which used the heel drop test, the results were compared to a professional system consisting of accelerometers made by PCB Piezotronics (model 353B33), a signal conditioner made by PCB Piezotronics (model 482A22), and a data acquisition module made by Linx (model ADS2000). The tests were used to evaluate the capacity of the data acquisition system in a specific frequency range (≈ 1.00 Hz – 37.83 Hz) equivalent to that of real structures, especially cable-stayed structures, which present structural problems due to excessive oscillations. In addition, it was possible to use usual sampling frequency values for testing civil engineering structures (around 200 Hz). All experiments presented promising results. For the tests with one sensor, the maximum difference in the natural frequencies identified compared to a professional accelerometer was 2.41%. The test using two sensors also enabled the identification of three mode shapes, and a maximum difference in the natural frequencies of 4.30% was obtained (related to the third mode shape). More details about the validation of the proposed data acquisition system can be found in [17].

### 3.2 The footbridge

The cable-stayed footbridge crosses the BR101 highway at km 88, in the city of Nossa Senhora do Socorro, Sergipe State, Brazil. The deck is 58.0 m long and 2.0 m wide, divided into two parts by a single central mast 22.4 m tall. The semi-fan cable arrangement of the bridge is distributed spatially in two inclined planes on each side of the deck. Each plane has eight stay cables. Half of the 16 cables are backstays, anchored externally to a foundation block (see Figure 2a). All of the stays use 32 mm-diameter Dywidag bars and the superstructure concrete has fck = 30 MPa (design value). Problems with the foundations of the structure resulted in unexpected deformation of the mast and deck. This problem was resolved, but the footbridge displays excessive oscillations in service under usual loads (pedestrians crossing and wind). These were factors that encouraged this research to be undertaken.

A 3D finite element model of the footbridge was created for this study using SAP2000 software [26] (see Figure 2b). Six-degree-of-freedom single beam elements at each end were used for the deck and tower, and cable elements were used for the stay cables, totaling 349 beam elements, 16 cable elements, 468 nodes, and 2808 degrees of freedom. Specifically, four 3D beam elements with equivalent stiffness were used for the deck. The cross-section was divided into four parts; the moment of inertia and the centroid showing the longitudinal equivalent element positions were calculated for each part. The stiffness of transverse elements was calculated for the 0.5 m half-widths between them (3D beam elements were also used). For the tower, 3D beam elements considering the design cross-section were used

and, for the stay cables, cable elements with undeformed lengths. The concrete weight per unit volume was assumed to be 25.0 kN/m$^3$ and the modulus of elasticity to be 30 GPa. The cable (Dywidag bar) weight per unit volume provided by the manufacturer was 76.9415 kN/m$^3$ and the modulus of elasticity was 205 GPa. The boundary conditions between the deck and tower, the deck and anchorage block, and the tower and foundation were considered fixed for rotations and displacements. The pylon support was assumed to be fixed for displacements only, as well as the connection between the stay cables and the anchorage block. The numerical model, used here only to define the test setups through the theoretical mode shapes and to evaluate the experimental results, presented perfect contact and sliding boundary conditions, which can be calibrated using the dynamic properties extracted experimentally.

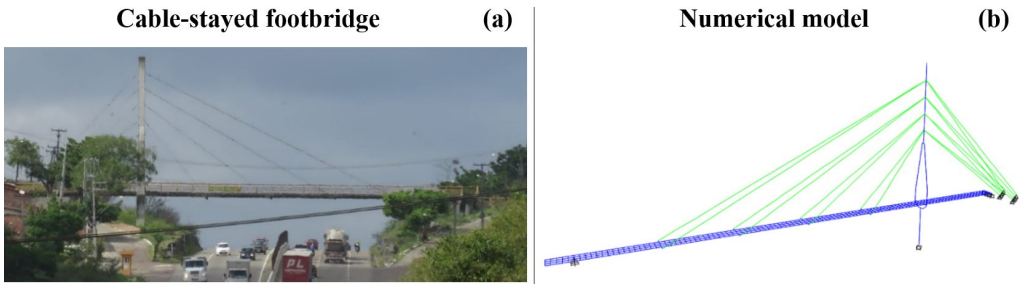


**Figure 2. (a)** Cable-stayed footbridge, Sergipe, Brazil; **(b)** Numerical model.

### 3.3 Field test routine

The excitation types cited in the literature for the various tests conducted on footbridges during experimental analysis result from shock, slow sine sweep testing, ambient vibration (normal operating conditions), and pedestrian walking and jumping [27]-[29]. Although there are several modal test techniques available for footbridges, those that require investigation are generally lightweight, with natural frequencies of less than 5 Hz, and can be excited with high energy for the designed load, such as pedestrians crossing. Consequently, the response generated by pedestrians walking or jumping is widely used in footbridge dynamic testing [28]. For stay cables, a range of techniques with different sensors have been used, i.e., lift-off test, electromagnetic sensor method, and vibration method (using accelerometers, laser interferometry, Ground-based Microwave Interferometer, etc.) [30]-[32].

In addition to people crossing, the main excitation factors during the tests were wind and air displacement caused by trucks driving by under the footbridge, which remained quite stable during the testing period. Additionally, during the complete structure tests two people ran and jumped along the footbridge deck to increase the excitation energy. The 205 Hz sampling frequency lasted for 30 s, with a total of 6150 acceleration samples in g scale measured by three sensors fixed to the structure with scotch tape. The same procedure was used as in the acquisition system validation tests (surface cleaning and sensors protected by acrylic case, fixed directly to the structure). Despite the rule of thumb presented in the dynamic testing literature, the 30 s time window was adopted as a result of a limitation detected in the data acquisition system. The number of recorded samples varied for intervals longer than 30 seconds, even while using the same codes for the three boards, which affected the synchronization of the obtained data. In a previous evaluation, a relationship was identified between the measured data volume (sampling frequency), number of connected boards, and the computer processing power. This problem was not crucial to the case study but will be thoroughly investigated in the future.

The tests of the complete structure were conducted using 17 setups along the deck and mast. For each test setup, one board was used as a stationary sensor and two boards as mobile sensors. The stationary sensor (Arduino board 1) was positioned in the connection region of the deck with the stay cable 3 at left (S3-L). It was defined as a reference measurement point for all test setups for calibrating energy content and normalizing signals. Based on analysis of the mode shapes provided by the numerical model of the footbridge), the position proved to be promising as it presents significant coordinates in almost all theoretical mode shapes. The pair of mobile sensors (Arduino boards 2 and 3) moved through 34 other measurement points, resulting in 17 test setups. The Arduino boards were synchronized by recording the computer operating system time in the board output. Although the accelerations were recorded in three directions, significant energy content was only generated perpendicularly to the structural elements. Therefore, only the z-direction in the deck and y-direction in the mast were considered in the system identification process. Figure 3 shows the test setups used in the Operational Modal Analysis (OMA).

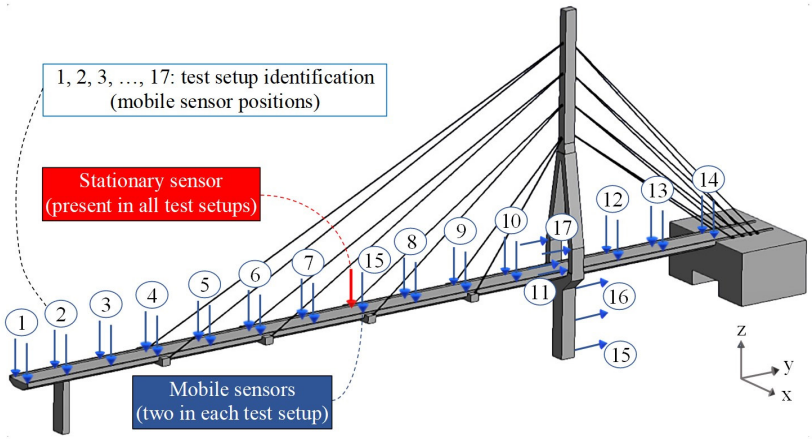


**Figure 3.** Test setups.

The excitation energy in the stay cables was increased by manually-imposed random initial displacements, while an Arduino board placed 2.0 m from the deck and fixed to the stay with a clamp measured the accelerations. The position chosen permitted identification of a minimum of four mode shapes. The 210 Hz sampling frequency lasted 30 s, with a total of 6300 acceleration samples on g scale. Figure 4 shows the test scheme and the proposed data acquisition system installed on-site, these examples are from Test setup 9 (global tests) and stay cable 2 at left (S2-L).

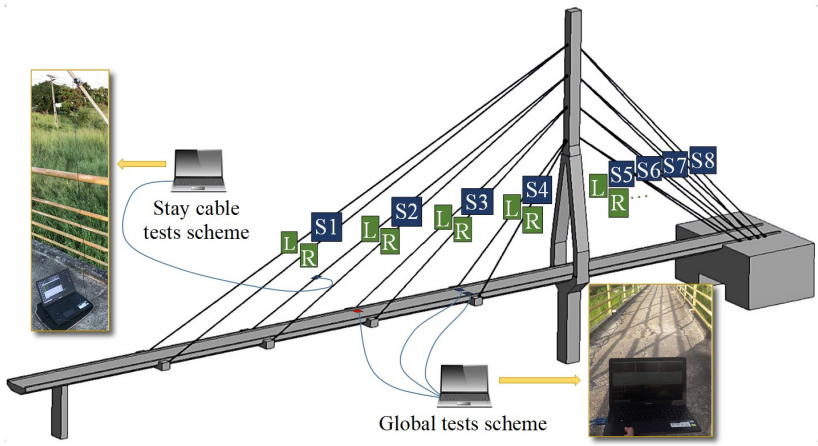


**Figure 4.** Data acquisition system installed on the footbridge – Global and stay cable tests.

## 4 RESULTS AND DISCUSSIONS

The experimental results of this research are presented below. The proposed data acquisition system was used in the dynamic tests described above, with three dynamic identification methods applied. The dynamic properties identified using the system are compared with those obtained with a 3D finite element model.

### 4.1 Stay cables

Stay cables are one of the most critical structural components in cable-stayed structures, since cable tension plays an important role in the construction, control, and monitoring of these structures [33]. The cable's natural frequencies were identified using the PP method. The spectral information presented below was obtained through the equations described in section 2.1, which were implemented in this research using the Matlab software [34]. Figure 5a shows the acceleration time series of the stay cable 2 at left (S2-L) (see Figure 4) obtained with the Arduino board, and Figure 5b shows the signal power spectrum.

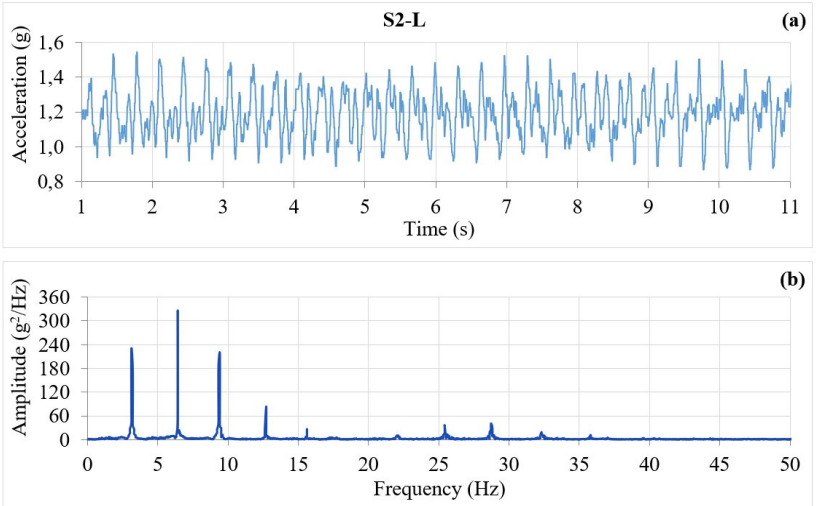


**Figure 5. (a)** Acceleration time series of the S2-L stay; **(b)** signal power spectrum.

It is interesting to note the high energy of the second peak, which can be explained by the position of the sensor. For the stays S2 (at left and right), the region where the board was positioned has the highest coordinates of the second theoretical mode shape. The cable's natural frequencies were used to determine the on-site axial forces of the stays. A simple way to estimate the cable forces in terms of natural vibration frequencies is to use the Vibrating String Mersenne/Taylor Law, considering that the cable is pinned at both ends, given by Equation 12:

$$f_n = \frac{n}{2L}\sqrt{\frac{T}{m}} \tag{12}$$

where $n$ = mode shape number; $L$ = cable span; $T$ = cable force; $m$ = mass per unit cable length; and $f_n$ = natural frequency of the $n$ mode shape.

The cable length was obtained from the solid drawing, i.e., it is the length between the concrete element faces. Table 1 shows, for example, the stay cable axial forces related to the 1st, 2nd, 3rd and 4th natural frequencies obtained for the stays 1, 2 and 3 (at left and right) through the PP Method.

**Table 1.** Stay cable forces related to the first four natural frequencies (S1, S2 and S3).

| Stay cable | 1st frequency (Hz) [related force (kN)] | 2nd frequency (Hz) [related force (kN)] | 3rd frequency (Hz) [related force (kN)] | 4th frequency (Hz) [related force (kN)] | Average force (kN) |
|---|---|---|---|---|---|
| S1-L | 2.733 [226.935] | 5.465 [226.852] | 8.397 [238.028] | 11.030 [231.022] | **230.710** |
| S1-R | 2.799 [238.028] | 5.564 [235.146] | 8.530 [245.628] | 11.230 [239.476] | **239.570** |
| S2-L | 3.125 [174.954] | 6.383 [182.479] | 9.376 [174.991] | 12.670 [179.745] | **178.042** |
| S2-R | 3.128 [175.290] | 6.323 [179.064] | 9.284 [171.574] | 12.550 [176.356] | **175.571** |
| S3-L | 4.420 [173.207] | 8.807 [171.916] | 13.560 [181.133] | 17.850 [176.554] | **175.703** |
| S3-R | 4.504 [179.853] | 8.976 [178.578] | 13.810 [187.874] | 18.150 [182.539] | **182.211** |
| ⋮ | ⋮ | ⋮ | ⋮ | ⋮ | ⋮ |

## 4.2 Complete structure

The dynamic properties, natural frequencies, and mode shapes were identified from ambient vibration data using the FDD and SSI-UPC methods. These are available in the ARTeMIS Modal 4.0 software [35], which was used in this section of the research. The accelerations were recorded and it was observed that the system's 0.01g limitation interfered with the acquisition of intervals with low variation of acceleration, resulting in levels in the time series. This problem was overcome by applying the moving average concept. In the case of the signals from the monitored footbridge, a moving average time frame of seven samples was sufficient. Figure 6a shows the recorded and "improved" acceleration

time series, using the example of Test Setup 9, and Figure 6b shows the moving average applied to the Mobile sensor 1 signal, between 11 and 22 seconds. The raw signal is in black and "improved" signal is in blue.

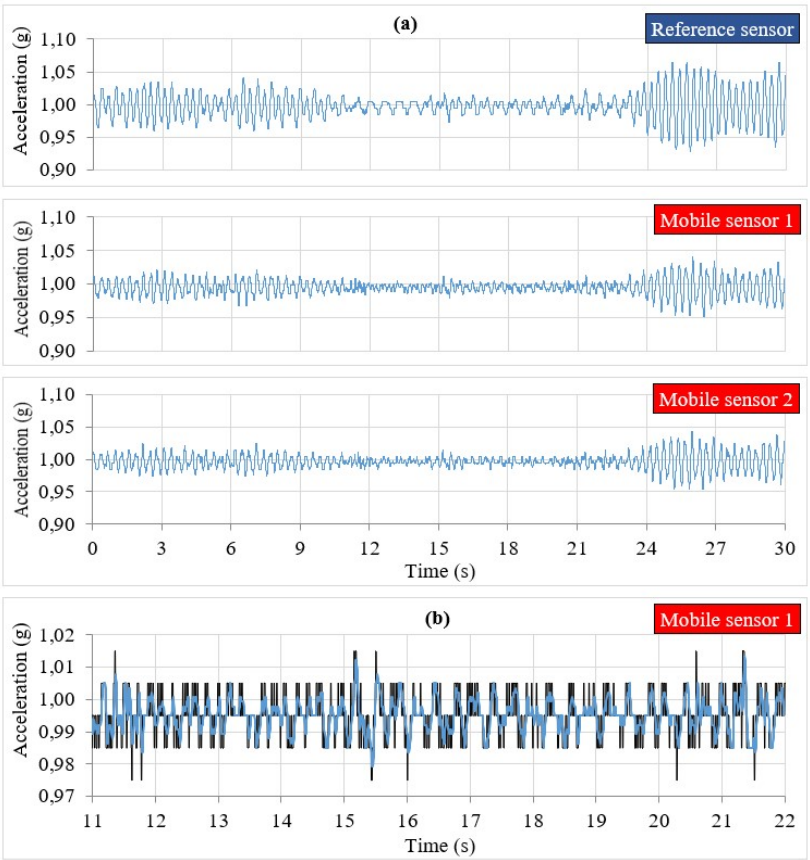


**Figure 6. (a)** Acceleration time-series captured by the data acquisition system in Test Setup 9; **(b)** Detail of the moving average applied to the signal.

Figure 7 shows the average normalized PSD function of the signals shown in Figure 6 decomposed into three singular values (SVD 1, SVD 2 and SVD 3) using the FDD method.

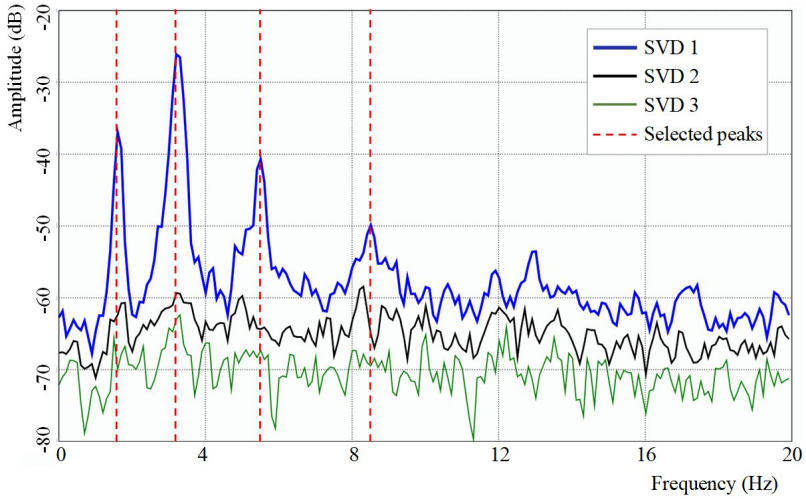


**Figure 7.** Average normalized PSD function decomposed into three singular values, using the FDD (Test setup 9).

The spectrum shows four well-defined peaks, highlighted in Figure 7. These peaks represent the first four natural frequencies related to the footbridge's first four flexural mode shapes. Table 2 shows the natural frequencies identified by the FDD method and compares the values and mode shapes with the numerical model using the Modal Assurance Criterion (MAC). The MAC index shows the correlation between mode shapes. It can vary between 0 and 1, where values close to 0 correspond to a lack of correlation, while values close to 1 indicate consistent correlation between the mode shapes. In the case of this research, the index was calculated to show the correlation between the experimental and numerical (reference) mode shapes, using Equation 13 below:

$$MAC = \frac{|\varphi_{exp}^{T}\varphi_{num}|^{2}}{(\varphi_{exp}^{T}\varphi_{exp})(\varphi_{num}^{T}\varphi_{num})} \tag{13}$$

where $\varphi_{exp}$ = experimental modal vector; $\varphi_{num}$ = numerical modal vector; "$^{T}$" = vector transpose.

**Table 2.** First four flexural natural frequencies identified by the FDD.

| Flexural mode shape | $f_{FDD}$ | $f_{numerical\ model}$ | Difference | MAC |
|---|---|---|---|---|
| 1st | 1.6016 Hz | 1.6404 Hz | ↓ 2.37% | 0.9990 |
| 2nd | 3.2031 Hz | 3.2423 Hz | ↓ 1.21% | 0.9915 |
| 3rd | 5.5054 Hz | 5.4472 Hz | ↑ 1.07% | 0.8554 |
| 4th | 8.5083 Hz | 8.3444 Hz | ↑ 1.96% | 0.9068 |

The experimental process identified natural frequency values very close to those provided by the numerical model. The greatest difference between these values, of 2.37%, was observed in the first frequency, while in the other frequencies the difference was between 1 and 2%.

Figure 8 shows the stabilization diagram of the signals shown in Figure 6 for the estimated state-space mode, using the SSI-UPC method.

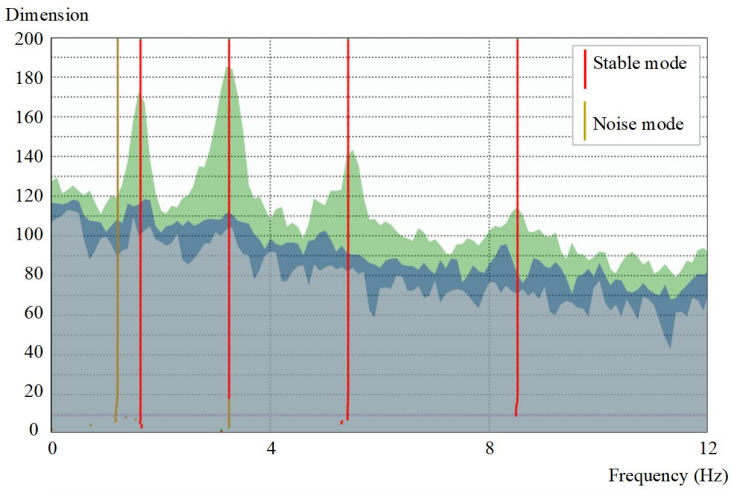


**Figure 8.** Mode shapes identified by the SSI-UPC (Test setup 9).

The SSI-UPC method highlighted five frequencies in the PSD function of the signals obtained in Test setup 9, decomposed into three singular values (SVD 1, SVD 2 and SVD 3). Four were classified as natural frequencies related to stable modes of vibration. The other, close to the first spectrum peak, was classified as related to a noise mode, probably resulting from the noisy signal of the acquisition system. Table 3 shows the natural frequencies related to the stable modes–in this case flexural mode shapes–identified by the method, and compares the results with the frequencies and mode shapes (MAC) provided by the numerical model.

**Table 3.** First four flexural natural frequencies identified by the SSI-UPC.

| Flexural mode shape | $f_{SSI\text{-}UPC}$ | $f_{numerical\ model}$ | Difference | MAC |
|---|---|---|---|---|
| 1st | 1.6315 Hz | 1.6404 Hz | ↓ 0.54% | 0.9971 |
| 2nd | 3.2479 Hz | 3.2423 Hz | ↑ 0.17% | 0.9895 |
| 3rd | 5.4139 Hz | 5.4472 Hz | ↓ 0.61% | 0.8513 |
| 4th | 8.4900 Hz | 8.3444 Hz | ↑ 1.74% | 0.9017 |

The experimental process identified natural frequency values very close to those provided by the numerical model. The greatest difference between them, of 1.74%, was observed in the fourth frequency, while in the other frequencies the difference was between 0.1 and 0.7%.

In general, the flexural modes identified presented excellent shapes. However, the third and fourth flexural mode shapes indicated problems in some coordinates (highlighted in Figure 9). Consequently, these presented the lowest MAC indexes among the identified mode shapes. The FDD method identified mode shapes with ≈ 0.86 and 0.91 MAC indexes, and the SSI-UPC method identified mode shapes with ≈ 0.85 and 0.90 MAC indexes, respectively. Analysis of all the measurement points and mode shapes obtained in previous tests [17] and in this case study suggests that this is due to the accuracy of the Arduino board (0.01g). The problem regions have the largest modal coordinates of the third and fourth theoretical modes of vibration. Experimentally, the acceleration variations in the adopted sampling frequency may not have been detected by the sensors, resulting in the signal saturation. On the other hand, the discontinuity of the third and fourth experimental modal vectors could be a warning of the existence of damage. This is an interesting possibility and will be part of a future study. Figure 9 shows the first four flexural mode shapes provided by the numerical model (Figure 9a) and experimentally identified by the proposed data acquisition system and FDD method (Figure 9b), and SSI-UPC method (Figure 9c).

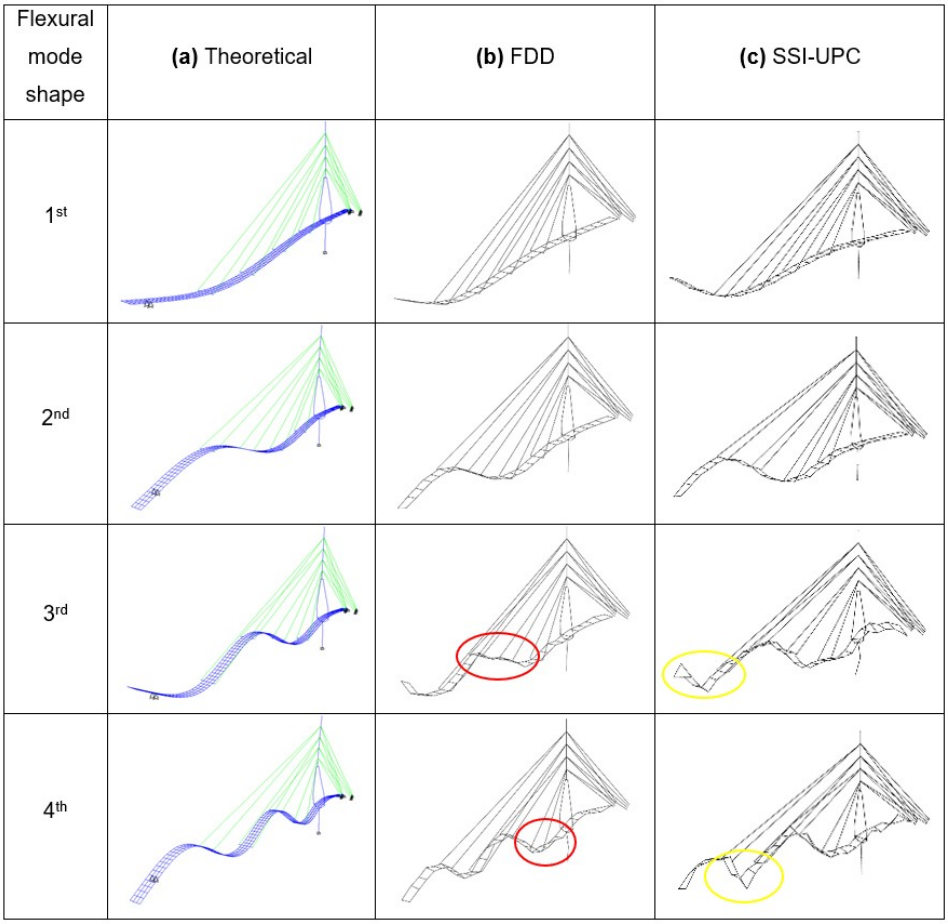


**Figure 9.** First four flexural mode shapes: **(a)** provided by the numerical model; **(b)** experimentally identified by FDD; **(c)** experimentally identified by SSI-UPC.

No transverse and torsional mode shapes were identified. Either it was difficult to generate enough energy in the corresponding directions during the tests or the respective vibrations were not noticeable, which explains the absence of these vibration modes in the system identification process.

## 5 CONCLUSIONS

The proposed system efficiently recorded the time series necessary for the OMA, with the acceleration acquisition process providing stable results in both the cable and complete structure tests. Despite the level of noise in the output signal revealed by the spectral density functions and the limited precision that made it difficult to capture low variations of accelerations, at least four mode shapes were identified in all tests. It was demonstrated that even with limited resources it is possible to obtain data for the evaluation of real structures.

The acceleration time series and the PSD functions were well-defined in all cable tests. At least four high energy peaks in the 0 – 24 Hz frequency range were generated by the data acquisition system and the PP method. These were used to determine the cable forces on-site. The procedure was effective, since the deck shape resulting from the numerical model resembled that observed visually on-site, which directly depends on the set forces of the stay cables.

In the tests of the complete structure, the data acquisition system and the identification methods were good tools for obtaining the first four flexural stable mode shapes, within the 0 – 9 Hz frequency range. Comparing the results to a 3D finite element model, the experimental natural frequencies presented a good correlation with the theoretical frequencies. When using the FDD method, the greatest difference, of 2.37%, was observed in the first frequency, while in the other frequencies the difference was between 1 and 2%. When using the SSI-UPC method, the greatest difference was 1.74% in the fourth frequency, while in the other frequencies the difference was between 0.1 and 0.7%. Despite the excellent shapes of the first and second experimental modes of vibration (MAC indexes above 0.99), the third and fourth flexural mode shapes indicated a continuity problem in some coordinates. The region has the largest modal coordinates in the respective theoretical mode shape. The acceleration variations may not have been detected by the sensors experimentally, resulting in signal saturation, or the discontinuity of the third and fourth experimental modal vectors may be indicating damage. A future study based on a damage detection routine will clarify this uncertainty and warn of any structural problems, if applicable.

In general, the proposed data acquisition system demonstrates the capacity to acquire the response time series used in the dynamic identification of civil engineering structures, but some improvements are necessary. Future research will seek to increase the accuracy of the system, if possible, to enable it to deal with structures that have low variations in acceleration (less than 0.01g). This would rule out the need to use the moving average. Another aspect is the synchronization of the devices. The number of records varies considerably for recording intervals longer than 30 seconds when using acquisition systems with multiple devices. Therefore, longer measurement time windows were avoided, despite the rule of thumb presented in the dynamic testing literature. It is very likely that other mode shapes will be identified if this problem can be overcome. Additionally, low-cost systems and sensors that have acceptable performance and close-to-optimal parameters for micro vibration detection, such as the one developed in this research, enable continuous and remote monitoring of the structure. This eliminates the need to interrupt the structure's operations and travel to the location. The Arduino boards were chosen for their portability, resistance, and cost. They could be fixed to and/or embedded in the structure (not recovered) to remotely record accelerations via wireless, especially with larger structures such as bridges, buildings, etc.

## ACKNOWLEDGEMENTS

The authors wish to thank DNIT for authorizing the tests, B. de Almeida for the photos of the footbridge, and A. Araujo and E. Nunes for their assistance in conducting the tests.

## REFERENCES

[1] W.-X. Ren and X.-L. Peng, "Baseline finite element modeling of a large span cable-stayed bridge through field ambient vibration tests," *Comput. Struc.*, vol. 83, no. 8-9, pp. 536–550, Mar 2005, http://dx.doi.org/10.1016/j.compstruc.2004.11.013.

[2] C. Chisari, C. Bedon, and C. Amadio, "Dynamic and static identification of base-isolated bridges using genetic algorithms," *Eng. Struct.*, vol. 102, no. 1, pp. 80–92, Nov 2015, http://dx.doi.org/10.1016/j.engstruct.2015.07.043.

[3] K.-V. Yuen, "Updating large models for mechanical systems using incomplete modal measurement," *Mech. Syst. Signal Process.*, vol. 28, pp. 297–308, Apr 2012, http://dx.doi.org/10.1016/j.ymssp.2011.08.005.

[4] A. Malekjafarian and E. J. Obrien, "Identification of bridge mode shapes using short time frequency domain decomposition of the responses measured in a passing vehicle," *Eng. Struct.*, vol. 81, no. 15, pp. 386–397, Dec 2014, http://dx.doi.org/10.1016/j.engstruct.2014.10.007.

[5] F. P. Pentaris, J. Stonham, and J. P. Makris, "A review of the state-of–the-art of wireless SHM systems and an experimental set-up towards an improved design," in *Proc. Eurocon 2013*, 2013, pp. 275-282, https://doi.org/10.1109/EUROCON.2013.6624997.

[6] Y. Liu and S. Nayak, "Structural health monitoring: state of the art and perspectives," *J. Miner. Met. Mater. Soc.*, vol. 64, no. 7, pp. 789–792, Jul 2012, http://dx.doi.org/10.1007/s11837-012-0370-9.

[7] C. Negulescu et al., "Comparison of seismometer and radar measurements for the modal identification of civil engineering structures," *Eng. Struct.*, vol. 51, pp. 10–22, Jun 2013, http://dx.doi.org/10.1016/j.engstruct.2013.01.005.

[8] J.-H. Weng, C.-H. Loh, J. P. Lynch, K.-C. Lu, P.-Y. Lin, and Y. Wang, "Output-only modal identification of a cable-stayed bridge using wireless monitoring systems," *Eng. Struct.*, vol. 30, no. 7, pp. 1820–1830, Jul 2008, http://dx.doi.org/10.1016/j.engstruct.2007.12.002.

[9] E. Toledo Júnior, A. Cury, and J. Landre Júnior, "Assessment of low-cost wireless sensors for structural health monitoring applications," *Rev. IBRACON Estrut. Mater.*, vol. 14, no. 2, pp. e14213, 2021, http://dx.doi.org/ 10.1590/S1983-41952021000200013.

[10] J. D. Braido and Z. M. C. Pravia, "Application of MEMS accelerometer of smartphones to define natural frequencies and damping ratios obtained from concrete viaducts and footbridge," *Rev. IBRACON Estrut. Mater.*, vol. 15, no. 2, pp. e15206, 2022, http://dx.doi.org/10.1590/S1983-41952022000200006.

[11] F. Khoshnoud and C. W. de Silva, "Recent advances in MEMS sensor technology – mechanical applications," *IEEE Instrum. Meas. Mag.*, vol. 15, no. 2, pp. 14–24, Apr 2012, http://dx.doi.org/10.1109/MIM.2012.6174574.

[12] M. Moradi and S. Sivoththaman, "MEMS multisensor intelligent damage detection for wind turbines," *IEEE Sens. J.*, vol. 15, no. 3, pp. 1437–1444, Mar 2015, http://dx.doi.org/10.1109/JSEN.2014.2362411.

[13] G. S. Maruthi and V. Hedge, "Application of MEMS accelerometer for detection and diagnosis of multiple faults in the roller element bearings of three phase induction motor," *IEEE Sens. J.*, vol. 16, no. 1, pp. 145–152, Jan 2016, http://dx.doi.org/10.1109/JSEN.2015.2476561.

[14] L. A. S. Pedotti, R. M. Zago and F. Fruett, "Fault diagnostics in rotary machines through spectral vibration analysis using low-cost MEMS devices," *IEEE Instrum. Meas. Mag.*, vol. 20, no. 6, pp. 39–44, Dec 2017, http://dx.doi.org/10.1109/MIM.2017.8121950.

[15] A. Vidal-Pardo and S. Pindado, "Design and development of a 5-channel arduino-based data acquisition system (ABDAS) for experimental aerodynamics research," *Sensors (Basel)*, vol. 18, no. 7, pp. 2382–2402, Jul 2018, http://dx.doi.org/10.3390/s18072382.

[16] A. González, J. L. Olazagoitia, and J. Vinolas, "A low-cost data acquisition system for automobile dynamics applications," *Sensors (Basel)*, vol. 18, no. 2, pp. 366–386, Jan 2018, http://dx.doi.org/10.3390/s18020366.

[17] D. S. Nunes, J.L.V. Brito and G.N. Doz, "A low-cost data acquisition system for dynamic structural identification," *IEEE Instrumen. Meas. Mag.*, vol. 22, no. 5, pp. 64-72, Oct. 2019, http://dx.doi.org/10.1109/IMM.2019.8868280.

[18] Arduino.CC, "Language Reference." Arduino.CC. https://www.arduino.cc/reference/en/ (accessed Jan. 8, 2022).

[19] Arduino IDE, "Arduino 1.8.5." Arduino IDE. https://www.arduino.cc/en/software (accessed Jan. 8, 2022).

[20] Arduino.CC., "What is Arduino?." Arduino.CC. http://www.arduino.cc/en/Guide/Introduction (accessed Jan. 8, 2022).

[21] G. Lockridge, B. Dzwonkowski, R. Nelson, and S. Powers, "Development of a low-cost arduino-based sonde for coastal applications," *Sensors (Basel)*, vol. 16, no. 4, pp. 528–544, Apr 2016, http://dx.doi.org/10.3390/s16040528.

[22] RealTerm software, "Realterm: serial and TCP terminal for engineering and debugging 3.0.1.44." http://realterm.sourceforge.io (accessed Jan. 8, 2022).

[23] B. Peeters, "System identification and damage detection in civil engineering," Ph.D. Thesis, Kath. Univ. Leuven, Belgium, 2000.

[24] J. Rodrigues, "Identificação modal estocástica – Métodos de análise e aplicações em estruturas de engenharia civil," Ph.D. Thesis, Fac. de Eng. da Univ. do Porto, Portugal, 2004.

[25] Arduino.CC., "Arduino 101." Arduino.CC. https://docs.arduino.cc/retired/boards/arduino-101-619 (accessed Jan. 8, 2022).

[26] Computers and Structures Inc., *SAP2000 Integrated Software for Structural Analysis and Design*. Berkeley, California: CSI – Computers and Structures Inc., 2000.

[27] R. Cantieni, "Cable-stayed footbridge: investigation into superstructure and cable dynamics," *Top. Dyn. Bridges*, vol. 3, pp. 11–25, Mar 2013, http://dx.doi.org/10.1007/978-1-4614-6519-5_2.

[28] J. M. W. Brownjohn et al., "Footbridge system identification using wireless inertial measurements units for force and response measurements," *J. Sound Vibrat.*, vol. 384, no. 8, pp. 339–355, Dec 2016, http://dx.doi.org/10.1016/j.jsv.2016.08.008.

[29] I. J. Drygala and J. M. Dulinska, "A theoretical and experimental evaluation of the modal properties of a cable-stayed footbridge," *Procedia Eng.*, vol. 199, pp. 2937–2942, 2017, http://dx.doi.org/10.1016/j.proeng.2017.09.347.

[30] L. O. Santos and X. Min, "Load Tests of a cable-stayed bridge in Coimbra, Portugal," *Struct. Eng. Int.*, vol. 17, no. 4, pp. 337–341, Nov 2007, http://dx.doi.org/10.2749/101686607782359146.

[31] S. Cho, J. Yim, S. W. Shin, H.-J. Jung, C.-B. Yun, and M. L. Wang, "Comparative field study of cable tension measurement for a cable-stayed bridge," *J. Bridge Eng.*, vol. 18, no. 8, pp. 748–757, Aug 2013, http://dx.doi.org/10.1061/(ASCE)BE.1943-5592.0000421.

[32] G. Piniotis, V. Gikas, T. Mpimis, and H. Perakis, "Deck and cable dynamic testing of a single-span bridge using radar interferometry and videometry measurements," *J. Appl. Geod.*, vol. 10, no. 1, pp. 87–94, Jan 2016, http://dx.doi.org/10.1515/jag-2015-0030.

[33] J. Lardies and M.-N. Ta, "Modal parameter identification of stay cables from output-only measurements," *Mech. Syst. Signal Process.*, vol. 25, no. 1, pp. 133–150, Jan 2011, http://dx.doi.org/10.1016/j.ymssp.2010.05.020.

[34] Matlab, *Version R2017a. The MathWorks*, Inc – MATLAB and Simulink for Technical Computing.

[35] Structural Vibration Solution A/S, *ARTeMIS Modal 4.0. Ambient Response Testing and Modal Identification Software ARTeMIS Extractor Pro 4.0*. Aalborg East, Denmark: Structural Vibration Solution A/S.

**Author contributions:** DSN: conceptualization, methodology, data curation, writing; JLVB: data curation, formal analysis; GND: data curation, formal analysis.

**Editors:** Sergio Hampshire C. Santos, Guilherme Aris Parsekian.